Water Science & Technology

IWA PUBLISHING

Water Science & Technology Vol 88 No 6, 1608 doi: 10.2166/wst.2023.293

Facile fabrication of organic superhydrophobic corn silk-derived cellulose acetate nanofiber for the effective sequestration of oil from oil–water mixture

Sivashankar R* and Anand Kishore K

Department of Chemical Engineering, National Institute of Technology, Warangal, India
*Corresponding author. E-mail: rsivashankar@ymail.com

SR, 0000-0003-2380-117X

ABSTRACT

Oil spills and subsequent cleanup by oil–water separation remain a global concern. For the first time, corn silk-derived cellulose acetate (CSCA) and polyacrylonitrile (PAN) composite nanofiber are reported to create a superhydrophobic oil–water sequestration membrane. CA : PAN solutions with various PAN concentrations were evaluated for viscosity and conductivity. A CSCA nanofiber membrane was fabricated through electrospinning, which was superhydrophobic and oleophilic in water. Scanning electron microscope, energy-dispersive spectroscopy, Fourier transform infrared spectroscopy, X-ray diffraction, and thermogravimetric analysis/differential scanning calorimetry were used to analyze the membrane's morphological features. CSCA nanofibers formed a highly spherical bead with a maximum contact angle of 156° (>120°) in pure water solutions, demonstrating their superhydrophobicity. This study found that membranes can remove oil from oil–water mixtures and emulsions, as gravity is the only force required for propelling the system. Mineral oil had the highest oil sorption capability (908%), while toluene had the lowest (664%). For mineral oil–water mixtures, the CSCA membrane has the greatest separation flux at a maximum of 442 L/m^2/h and the best separation efficiency at up to 99.67%. These findings provide strong support for using an as-prepared CSCA nanofiber membrane as a viable reusable oil sorbent in oil spill cleaning.

Key words: corn silk cellulose acetate, nanofiber, oil–water sequestration, superhydrophobic membrane

HIGHLIGHTS

- Organic eco-friendly corn silk-derived cellulose acetate (CSCA) nanofiber was fabricated.
- CSCA nanofiber featured exceptional oil–water separation capabilities.
- The CSCA nanofiber exhibited superior durability and recyclable qualities.
- With a separation efficiency of 99.67%, membranes are both superhydrophobic and oleophilic.

1. INTRODUCTION

The oil sector is a key supporter of economic and social advancement in modern civilization (Bai *et al.* 2023). The rapid development of industry has led to an increase in both the regularity of oil spills and the vast release of wastewater containing oil, both of which have become global environmental hazards that put both humans and aquatic organisms in danger (Ye *et al.* 2023). Separation methods for oil–water mixtures include centrifugation, adsorption, and flocculation, all of which have been shown to be effective in the past (Zhou *et al.* 2022). Because the water-in-oil emulsions with droplet sizes below 20 μm are more stabilized, these technologies are best for separating immiscible water-in-oil but challenging for separating water-in-oil emulsions (Kou *et al.* 2021). Furthermore, these techniques are plagued by secondary contamination, high costs, and poor separation efficiency (Ge *et al.* 2018). Separation methodology employing superhydrophobic membranes could be developed to successfully extract oil from water (Li *et al.* 2019). As a result, the development of novel materials as a means of achieving oil–water separation in a manner that is kind to the environment is of the utmost importance (Ye *et al.* 2023). In order to separate oil–water emulsions, researchers were devoted to creating superhydrophobic membranes, which had been motivated in part by the hydrophobic nature of leaves, butterfly wings, and spider silk (Zhang *et al.* 2019). Oil from an emulsified oil–water aqueous system can be isolated using materials like manufactured inorganic mineral substances, fiber-based materials,

and polymers that are organic in nature. When choosing the optimal sorbent material for oil removal, it is essential to prioritize high absorption capacity, hydrophobicity, and oleophilicity, in addition to strong recoverability (Wang *et al.* 2016). There is a substantial threat to the environment, the recyclability, and the long-term viability posed by treatments composed of inorganic particles and synthetic compounds. Inorganic particles and synthetic compounds are neither renewable nor biodegradable, posing a significant threat to the environment and social welfare. According to the findings of studies, there are a number of different materials that are capable of achieving hyperhydrophobicity. These materials include biodegradable polymers, cellulose, chitosan, and plant waxes. Recent years have witnessed a substantial quantity of research on natural organic materials, including the use of Mj-fiber (Wang *et al.* 2020c), duck down fiber (Fang *et al.* 2022), cellulose nanofiber (Shu *et al.* 2020), flax fibers (Liu 2020), jute fibers (Kovačević *et al.* 2023), kapok and waste cotton (Singh *et al.* 2023), and luffa sponge (Alvarado-Gómez *et al.* 2021). Although most of the natural and organic fiber materials are biodegradable, few of those can absorb water as well as oil, which reduces the effectiveness of separation and some others, and can sink during separation in rough sea conditions (Elmaghraby *et al.* 2022). Nanofibers are prepared by electrospinning, which is a simple and efficient technique that produces large specific surfaces (Xue *et al.* 2019). The resulting electrospun nanofiber mats are noteworthy because they exhibit highly interconnected porous nanostructures, exceptionally large specific surface areas, and a modifiable nature, and hence, this approach provides a fantastic way to make distinctive wettable surfaces (Mahmoud 2020). When compared to other fabrication methods, electrospinning stands out due to its flexibility in producing fibres with a wide variety of arrangements (such as aligned fibres, random orientations, or their combinations) and morphological structures (such as tubular scaffolds, flat surfaces, and asymmetrical configurations). The technique of making solid threads from solution does not necessitate the use of coagulation chemicals or high temperatures. Because of this, the method excels in producing fibres from huge and complicated compounds (Islam *et al.* 2019).

One of the most abundant and durable biopolymers in the earth is cellulose, which can be feasibly converted into the lucrative derivatives of cellulose acetate (CA) that has a variety of industrial applications (Nemr *et al.* 2017). Cellulose has a wide range of desirable characteristics, including low cost, biocompatibility, biodegradability, and chemical modifiability (Ma *et al.* 2016). The field of nanofibers has seen growing attention in CA (which is an acetate ester of cellulose) over the past decade. CA is frequently employed as an alternative to cellulose substitution due to cellulose's poor solubility in common solvents (Eleryan *et al.* 2021). Wheat straw, corn husk, rice hulls, sugar cane bagasse, rice husk, bamboo pulp, bamboo bark, coconut fiber, cotton tree, sugarcane bagasse, *Pinus* sp. sawdust, and many other agricultural wastes are some of the biomasses that have been utilized as raw material to create CA (Biswas *et al.* 2006; Israel *et al.* 2008; Embong *et al.* 2021; Trejo *et al.* 2022).

In this investigation, we sought to develop a novel, environmentally friendly CA nanofiber synthesized from corn silk (CS) for the purpose of recovering oil from oil–water emulsion. Since CS was not extensively researched for its environmental applications, it was decided to examine using CS to create extremely hydrophobic organic fiber. In the current study, CA has been synthesized into nanofibers (membranes) from CS to boost its ability to dissolve and hydrophobicity, as well as to facilitate electrospinning into nanofiber membranes for oil–water sequestration. The as-prepared CS-derived CA (CSCA) membrane was characterized using scanning electron microscope (SEM), Fourier transform infrared spectroscopy (FTIR), X-ray diffraction (XRD), energy-dispersive spectroscopy (EDS), and thermogravimetric analysis/differential scanning calorimetry (TGA/DSC) for analyzing their morphological features. Wettability characteristics in response to water and oil were analyzed using water contact angle (WCA) measurement. The viscosity and the conductivity of PAN solutions of varying concentrations were measured and analyzed. The ability of the as-prepared CSCA membrane was evaluated for its capacity to effectively isolate oils from oil–water mixtures as well as oil–water emulsions. Concurrently, the oil-sorbed sorbent, which could be reconstituted for several life cycles after being cleaned with 100% ethanol, was assessed.

2. MATERIALS AND METHODS

The CS residue that was used came from the agricultural cooperatives in the Warangal region, India. All chemicals and reagents employed in this study were analytical grade.

2.1. Cellulose extraction from corn silk

Employing an integrated green pretreatment that has been documented in the literature, cellulose has been extracted from dried CS (Araujo *et al.* 2019). Treatment with hot water was used in the first stage of a two-step procedure, which was then followed by treatment with a diluted NaOH solution. The treatment with hot water was conducted at a temperature of 190 °C for 30–40 min while undergoing constant mechanical stirring in a cylindrical reactor made of stainless steel with

a rough capacity of 2.5 L with a 10% w/v material feed loading rate. The substances that were insoluble were collected shortly after this treatment, completely rinsed in deionized water, and then desiccated at 60 °C. After being treated with hot water, the CS was then steeped in NaOH (2 wt%) at 80 °C for 12 h while being stirred magnetically. After being treated with alkali, the CS was scrubbed and repeatedly rinsed with deionized water until it became colorless. The final product was stored after having been dried at 60 °C.

2.2. Acetylation of cellulose

Despite the fact that cellulose and CA are thermoplastic polymers, cellulose's tight ordering renders it insoluble in organic solvents and prevents it from flowing when heated. However, CA may be fluidized by heat and dissolves in certain organic solvents. CA was produced from cellulose obtained from CS using acid treatment with slight modification that has been reported (Asriza *et al.* 2021). The extracted cellulose was mixed with 25–30 mL of glacial acetic acid and agitated continuously for 1 h at room temperature (RT) to form activated cellulose. About 15–20 mL of anhydride acetic acid and 3–5 drops of concentrated H_2SO_4 were combined in a separate container at 0 °C. The preceding solution combination had this solution mixture added to it, and then it was agitated mechanically for 3 h at a temperature of 45 °C. After 24 h of stirring at RT, we added 25 mL of 60% glacial acetic acid to the solution mixture in a drop-by-drop fashion. All of the solution was filtered through a Hoover. The resulting product was dripped with demineralized water several times until the pH reads neutral and also to obtain a white polymer precipitate. Gel permeation chromatography (GPC) determined that the molecular weight (M_n) of the final product, CA, was between 30,000 and 50,000. Furthermore, the produced CA was dried at 40 °C in a vacuum oven.

2.3. Electrospinning of CSCA

An electrospinning solution was prepared using CSCA and polyacrylonitrile (PAN, mol. wt. 150,000) at 12% (w/v) using a solvent of dimethylformamide (DMF). To prepare a 12% CA electrospinning solution, an appropriate amount of CSCA and PAN in the ratio of 3 : 1 was added to the DMF solvent. To create a uniform CA electrospinning solution combination, the mixture was swirled vigorously for 24 h under magnetic stirring at 45 °C. The electrospinning solution had been loaded into a 15 mL syringe (with a 22 gauge blunt needle as the spinneret). During the electrospinning process, the voltage was set at 20 kV, the distance across the tip of the needle and the collector was 15 cm, the injection rate remained set at 1 mL/h, the electrospinning period was set at 10 h, and the humidity was set at 40%. The temperature was set at ambient. The accumulation of viscous fluid during the electrospinning procedure causes the tip of the needle to become clogged, which undermines the jet, and also prevents fiber creation. In spite of the fact that there was no airflow throughout this part of the experiment, the needle tip had to be meticulously cleaned during each and every run of the spinning procedure so as to keep the fiber creation intact. After that, the fibrous mat that had accumulated on the aluminum foil was collected and preserved for later investigation.

2.4. CSCA nanofiber characterization

At RT, a Brookfield digital viscometer and a conductivity meter were used to measure the viscosity and conductivity of the CSCA and CA/PAN solutions, respectively. Electrospun CSCA nanofiber shape and diameter were investigated on a scanning electron microscope (TESCAN VEGA3 LMU). The contact measurements of the electrospun CSCA nanofiber were investigated using a contact angle goniometer (GBX Digidrop Goniometer). X-ray diffraction determined the CSCA nanofiber crystalline structure. To explore the interatomic characteristics of bonding and to examine the functional group existing in the produced CSCA nanofiber, FTIR (BRUKER ALPHA-II) analysis was conducted out in the wave number range of 400–4,000 cm^{-1}. In order to investigate the thermal degrading behavior of the CSCA nanofiber, thermogravimetric analysis techniques (Perkin Elmer TGA-7) were employed. An energy-dispersive X-ray analyzer (Shimadzu EDX-7000/8000) was also used to identify the individual elements comprising the CSCA nanofibers.

2.5. Oil sorption capacity

Oil sorption studies were conducted with five different oils (diesel, petrol, toluene, petroleum ether, and mineral oil) in this investigation. All of these oils were chosen for the experiment because of their non-polarity. Petroleum ether and mineral oil are both composed of aliphatic hydrocarbons, but diesel and petrol are likewise composed mostly of hydrocarbons, making them non-polar; toluene, on the other hand, is composed of C–C and C = C, which also makes it non-polar. Nanofiber substrates of a given weight were typically saturated by being submerged in 50 mL of various oils at RT for about 20 min. The

equation that might be used to determine the oil sorption capacity (Q, %) is as follows (Chen *et al.* 2022):

$$Q\ (\%) = \frac{M_a - M_b}{M_b} \times 100 \tag{1}$$

where the weight of the membrane before the oil sorption is denoted by M_b (g), and M_a (g) represents the membrane weight after the oil sorption.

2.6. Oil–water mixture sequestration study

The oil–water mixture was separated using a cross-flow filtration system with a diameter of 47 mm on a lab scale. For this research, a CSCA nanofiber membrane was tailored specifically for a 47 mm diameter circular wafer which was used for the filtration system. About 50 mL of an oil–water mixture (1:1 v/v) was created by mixing 25 mL of oil colored with solvent yellow 14 and 25 mL of methylene blue-colored water. For this study, diesel, petrol, toluene, petroleum ether, and mineral oil were employed to evaluate the separation flux and the efficiency of CSCA nanofiber membranes. To ensure that the membrane would come into touch with the oil and water phases, the separation mechanism was set at an angle of 45°. All filtering processes relied only on the force of gravity. Following is the formula that was used to determine the oil–water separation efficiency (E_s) of the membrane (Chen *et al.* 2022):

$$E_s = \frac{W_b}{W_a} \times 100\% \tag{2}$$

The water phase weight before the oil–water separation process is denoted by W_b (g), while the water phase weight after the procedure is denoted by W_a (g).

2.7. Oil–water emulsion sequestration study

To evaluate the membrane's separation capacity, a range of oil–water emulsions (diesel–water (D : W), petrol–water (P : W), toluene–water (T : W), petroleum ether–water (E : W), and mineral oil–water (M : W)) were utilized as feed solutions. In order to create the oil-in-water (O : W) emulsions, 10 mg of Tween-80 and 1 mL of oil were added to 99.0 mL of water, and the mixture was then sonicated for 4 h. The apparatus used for separating oil–water emulsion was identical to the one described above in the oil–water mixture study. Before emulsion separation, the membrane was thoroughly wetted with distilled water. After passing the emulsion separation test during the recycling test, the membrane was cleaned with ethanol and dried in a vacuum oven in preparation for the subsequent cycle experiment. The following formula was used to get the membrane's separation flux J (L/m^2/h) (Chen *et al.* 2022).

$$J = \frac{V}{A \times t} \tag{3}$$

During the process of separating oil from water emulsion, V (L) indicates the volume of filtered oil in the duration of t (h) and A (m^2) denotes the area of the membrane through which the filtrate travels.

2.8. Regeneration of the oil-sorbed CSCA nanofiber membrane

When selecting a product, the extent to which it may be reused is one of the most crucial factors to take into account from a financial point of view. The aforementioned oil–water separation cross-flow filtration system was utilized to conduct 25 consecutive 5-min tests on the CSCA membrane to determine its recycling capability. After every cycle, the oil-saturated CSCA nanofiber membrane was collected, squeezed mechanically to extract as much of the oil as possible, and then washed many times in 100% ethanol to get rid of any lingering traces of oil.

3. RESULTS AND DISCUSSION

3.1. Rheology of the CSCA nanofiber

The morphology and electrospinning phenomena are both closely correlated with the rheological behavior, or viscosity, of CA solution. It is essential to have a sufficiently viscous solution in order for the polymer jet to commence; otherwise, droplets would arise as a result of the Rayleigh instability induced by surface tension. The viscosity of the solution is believed to

be proportional to the amount of polymer present. Nanofibers have a larger diameter when the solution's viscosity is higher. Electrospinning relies on the creation of fibres, which can only occur at a certain concentration. On the other hand, in electrospinning, polymer flow instability owing to the high cohesion of the solution prevents electrospinning at higher viscosities. In addition, the polymer beads grow in size, the average distance between them expands, and the resulting fibres' diameter grows as the solution viscosity rises. This is why viscosity is such an important factor in any electrospinning procedure. The tangling of polymer chains in a high-viscoelastic system is what makes for smoother fibers. Fiber jets cannot develop without the tangling of chains because of surface tension. In order to find the best concentration of CA solution and the impact of PAN addition on the CA mixture for electrospinning, the viscosity level of CA and CA/PAN mixtures was tested. The viscosity of the CA and CA/PAN solutions with varying concentrations of CA in the range of 8–20 wt% in the DMF solvent system is shown in Figure 1(a). The CA and CA/PAN solutions had comparable viscosities, and the incorporation of 5 wt% CA did not significantly affect these properties. When the concentration of CA solution was less than 12 wt%, adding PAN to the solution had a negligible impact on the viscosity. When the concentration of CA was more than 12 wt %, a rather quick rise in the viscosity of CA and CA/PAN was observed. During the electrospinning process, both the CA solution at 12 wt% and the CA/PAN solution at a ratio of 3 : 1 were highly stable and could be electrospun continuously in a DMF solvent.

In Figure 1(b), we see the effect of varying PAN concentrations (0.5, 1, 1.5, 2, 2.5, 3, 3.5, and 4) in a CA solution of 12 wt% on the solution's conductivity. At PAN concentrations >2.5 wt%, the conductivity rose rapidly from a rather stable range of 0.5–2.5 wt%. The addition of PAN at lower concentrations increased the mobility, but the charge of excess PAN induced an increase in repulsion in the CA/PAN solution when the PAN concentration was more than 2.5 wt%. Because there was no miscibility at higher concentrations >3 wt%, certain PAN molecules were not mixed with CA molecules and were found independently in the solution. Furthermore, the increased conductivity owing to excess PAN seems to induce the production of finer nanofibers.

3.2. Morphology of CSCA nanofiber

The images obtained from the SEM of the electrospun CSCA fiber with their average diameter and size distributions are shown in Figure 2(a) and 2(b), respectively. The electrospun CSCA nanofiber produced a fibrous network with an average diameter of 0.57 μm. Bead-free cylindrical and smooth fibers with submicron sizes made up the morphological structure. Subsequently, it was apparent that barely any PAN molecules were attached to the surface of the fibers. This finding demonstrated that the existence of a modest quantity of PAN had a negligible influence on nanofiber diameter. When a tiny quantity of PAN is applied to the CSCA nanofiber, the diameter of the nanofiber rises. The wettability of the CSCA nanofiber was also examined using blue-colored water (pH 7) and yellow-colored oil (mineral oil). Figure 2(c) displays the wettability of CSCA nanofiber in response to water and oil. After applying water (blue) and mineral oil (yellow) to the top surface of the

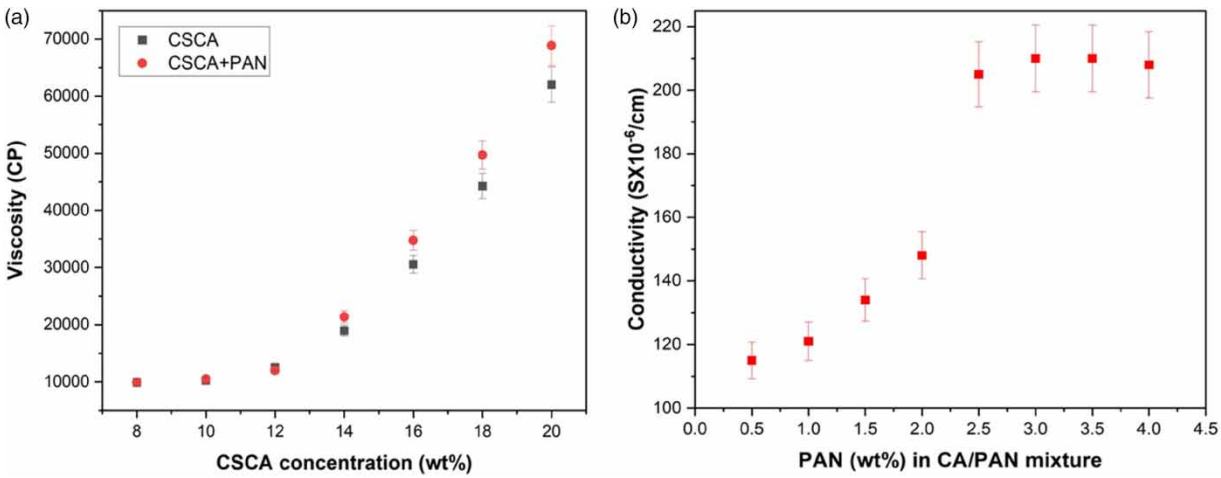

Figure 1 | (a) Viscosity determination at different CA concentrations. (b) Conductivity determination at varying PAN concentrations in a CA/PAN mixture.

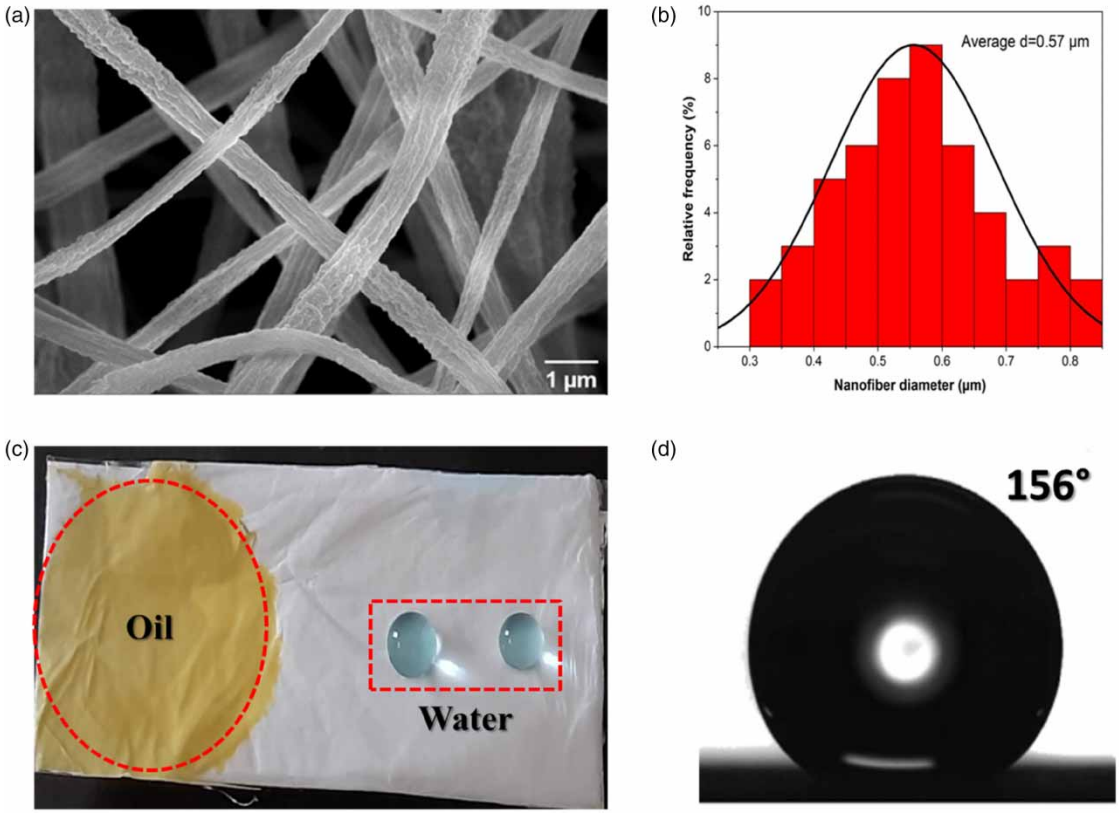

Figure 2 | Morphological characteristics: (a) SEM image of CSCA nanofiber, (b) size distribution of CSCA nanofiber, (c) wettability of oil and water on CSCA nanofiber, and (d) water contact measurement of CSCA nanofiber by a liquid (water).

CSCA nanofiber, the water droplet displayed an unchanged intact sphere shape on the surfaces, whereas the yellow mineral oil droplet was absorbed within the surrounding matrix. EDS elemental analysis revealed C, N, and O elements, confirming the existence of PAN and CA fibers in the membrane (Wang *et al.* 2020a). The weight %, atomic %, and elemental mapping of C, N, and O are presented in Figure 3(a). Figure 3(b) exhibits the FTIR spectra of CSCA nanofiber. From the figure, it is possible to attribute the absorbance peaks at 2,901 cm^{-1} to the C–H stretching vibrations of the CA and PAN units. A wide band peak in the CSCA nanofiber about 3,342 cm^{-1} was attributed to O–H stretching vibration. The inclusion of CA into the PAN matrix reduced the strength of the peaks at 1,605, 1,326, and 966 cm^{-1}, which are related to the $–OCOCH_3$ group in the CA unit. Bands about 1,421 cm^{-1} found ascribed to the C–H within the plane stretching vibrations. A broad band at 1,029 cm^{-1} was given for the C–O stretching of CA. FTIR clearly demonstrated that the CA and PAN fibers may have been physically linked to one another during the electrospinning process, and no chemical connection was created (Wang *et al.* 2020c; Elmaghraby *et al.* 2022). The XRD characteristics of CSCA nanofiber are displayed in Figure 3(c). The CA molecule can be identified by its two diffraction peaks located at $2\theta = 17.00°$ and 21.13° (Prakash *et al.* 2021). The crystalline structure of PAN may be deduced from the fact that it displayed a prominent diffraction peak with its center around 30.79°. In addition, research was conducted to determine the material's resistance to heat. Both the TGA and DSC curves of the CSCA nanofiber are displayed in Figure 3(d). The TGA curve illustrates various distinct stages in the process of sample deterioration. The first step of the process, which results in an enormous weight loss of more than 48% and takes place between temperatures of 260 and 280 °C, is the removal of moisture and volatile chemicals from the sample, as well as the beginning stages of cellulose and hemicellulose breakdown. When the temperature is higher than 290 °C, there is a continuing breakdown of CSCA. At temperatures between 320 and 520 °C, a further 18.56% of CSCA's mass was lost due to the breakdown and subsequent evaporation of related particles. The third phase saw a weight decrease of 24.30% around 520 and 640 °C (de Almeida *et al.* 2020). In addition, DSC testing between 50 and 600 °C verified the material's thermal resilience. Figure 3(d) shows that at 320 °C, CSCA reaches its endothermic peak as a result of the melting or breakdown of polysaccharides and celluloses (Sivashankar *et al.* 2022).

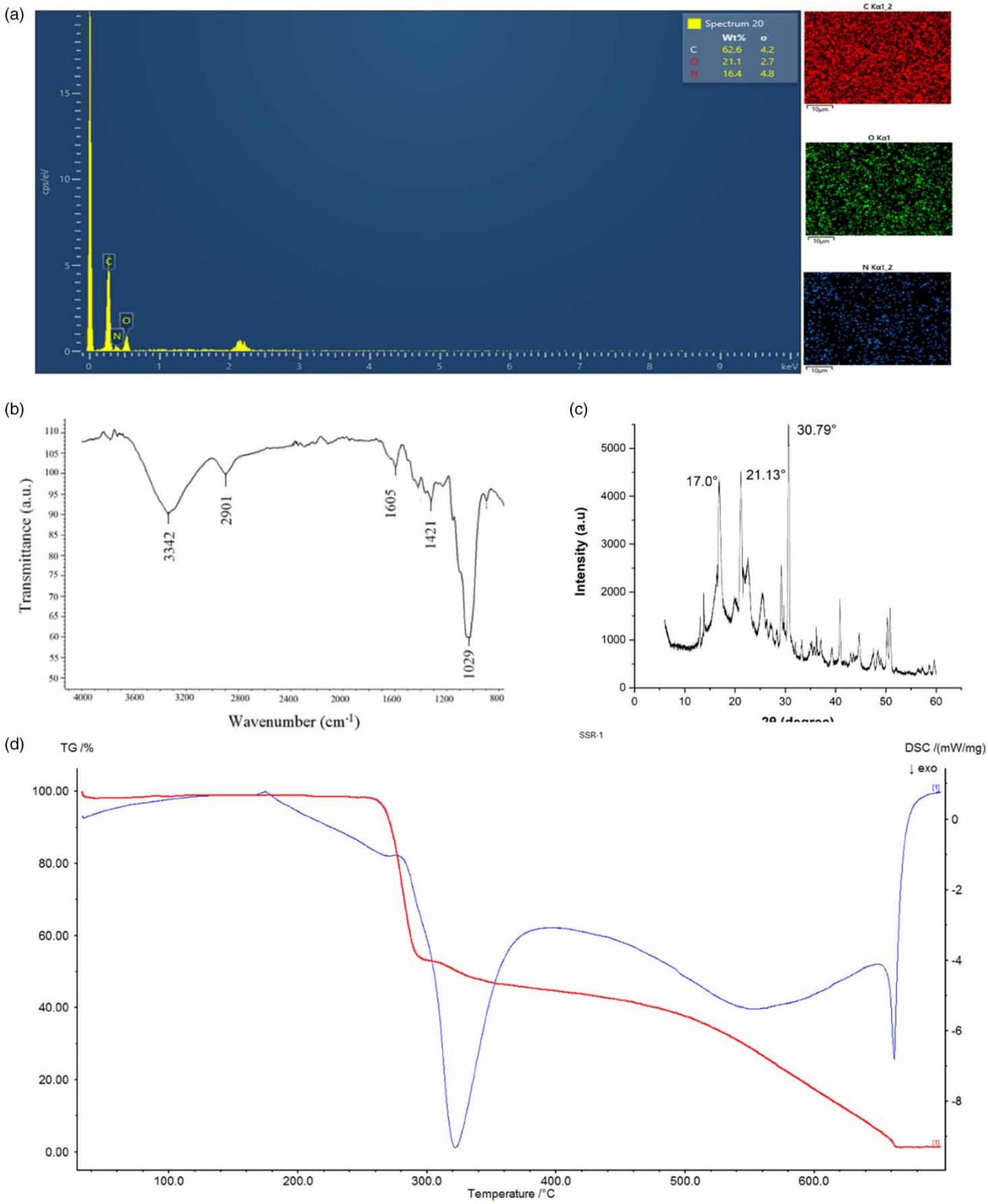

Figure 3 | (a) EDS image and mapping of C, N, and O elements in CSCA nanofiber, (b) FTIR spectra of CSCA nanofiber, (c) XRD analysis of CSCA nanofiber, and (d) TGA/DSC analysis of CSCA nanofiber.

3.3. WCA of CSCA nanofiber

In order to determine the wettability of electrospun CSCA nanofiber by a liquid that was made from 12% CSCA/PAN (3 : 1) solution in DMF, an examination of the WCA has been conducted. As-prepared CSCA nanofibers had a maximum contact angle of 156° (>120°) establishing a highly spherical bead, proving their exceptional superhydrophobicity in pure water solutions (Figure 2(d)). Figure 4(a) illustrates the results of a study on WCA measurement at various pH ranges (2–14). Furthermore, it came to light from Figure 4(a) that the WCA slightly increases from 139 to 154 as the pH rises from acid to neutral to alkaline, or from 2 to 14 pH, indicating that the CSCA nanofiber is appropriate for the sequestration of oil from oil–water mixture under an alkaline condition. Water droplets had a very low adhesion when forced to contact the sample surface, and almost no deformation was visible when they were forced to leave the surface. This extremely low adhesion could be attributed to the rough micro/nanostructure and a low surface energy substrate on the fabricated surface of CSCA nanofiber. Figure 4(b) shows the plot of the WCA of CSCA nanofiber against time for different pH values such as 2, 7, and 14. As a result of this study, it was possible to deduce that water droplets dispersed across the surface of the CSCA nanofiber membrane over the course of 100 s, demonstrating that the membrane possesses inadequate wetting capabilities.

3.4. Oil–water mixture sequestration

The effectiveness of the CSCA nanofiber in separating oil and water was examined. The experiment was conducted using an as-prepared CSCA nanofiber membrane immersed in water (blue-colored) and oil (yellow) under water as shown in Figure 5. Figure 5(a) indicates that a strong resistance of the CSCA nanofiber membrane to the absorption of water was demonstrated by the fact that it did not absorb any color from the colored water (blue) while being submerged in the water. From Figure 5(b), it could be visualized that the floating oil layer (yellow-colored mineral oil) may be easily removed from the water's surface and absorbed by a fragment of the CSCA nanofiber membrane, which then keeps the oil without leaking and submerged under water. The findings suggested that the CSCA nanofiber membrane has a high oil affinity for the quick removal of oil pollutants from underwater environments without allowing any oil to seep out. Furthermore, the experiments were conducted using a cross-flow filtration system with a diameter of 47 mm on a lab scale for oil–water mixture sequestration as shown in Figure 5(c). The filtration system was positioned at a 45° angle to the horizontal, so that the oil phase (lighter oil) could reach the filter membrane as it was floating above the water as reported in the literature (Chen *et al.* 2022). The water phase (blue) is entirely rejected from the top surface of the nanofiber membrane due to its high hydrophobicity and high porosity. On the other hand, the oil phase may readily infiltrate through the nanofiber membrane. The super lipophilic nature of the CSCA membrane caused an oily layer to grow on its surface during the separation process. This layer may serve as a means to stop water from passing through the CSCA membrane.

Figure 6(a) displays the results of oil sorption capacity. In this study, the oil sorption capacity for the as-prepared CSCA membrane was investigated using non-polar liquids such as diesel, petrol, toluene, petroleum ether, and mineral oil. In

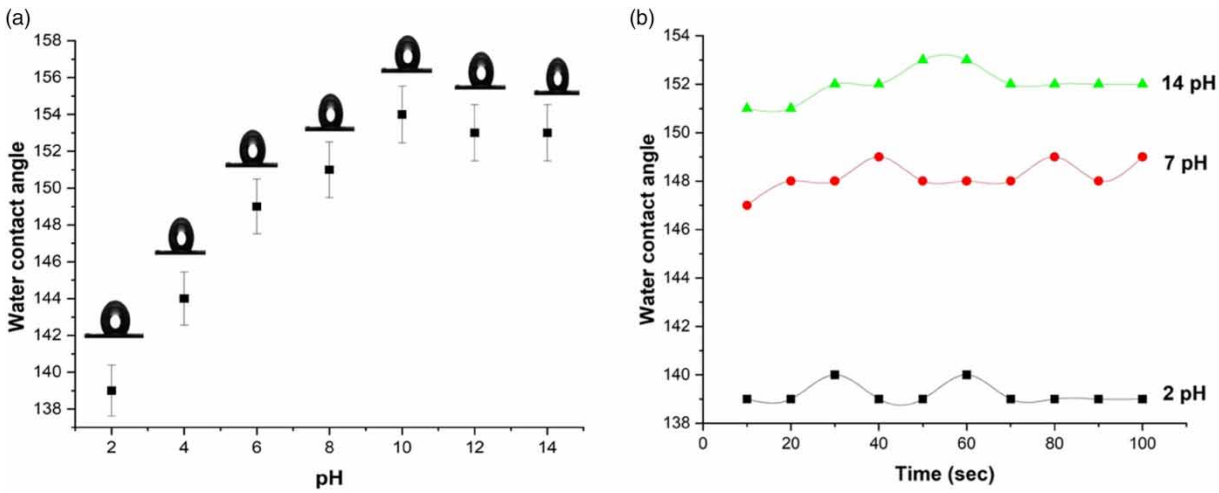

Figure 4 | (a) WCA measurements of CSCA nanofiber at different pH solution and (b) WCA measurements of CSCA nanofiber against time for acid (pH 2), neutral (pH 7), and alkaline (pH 14).

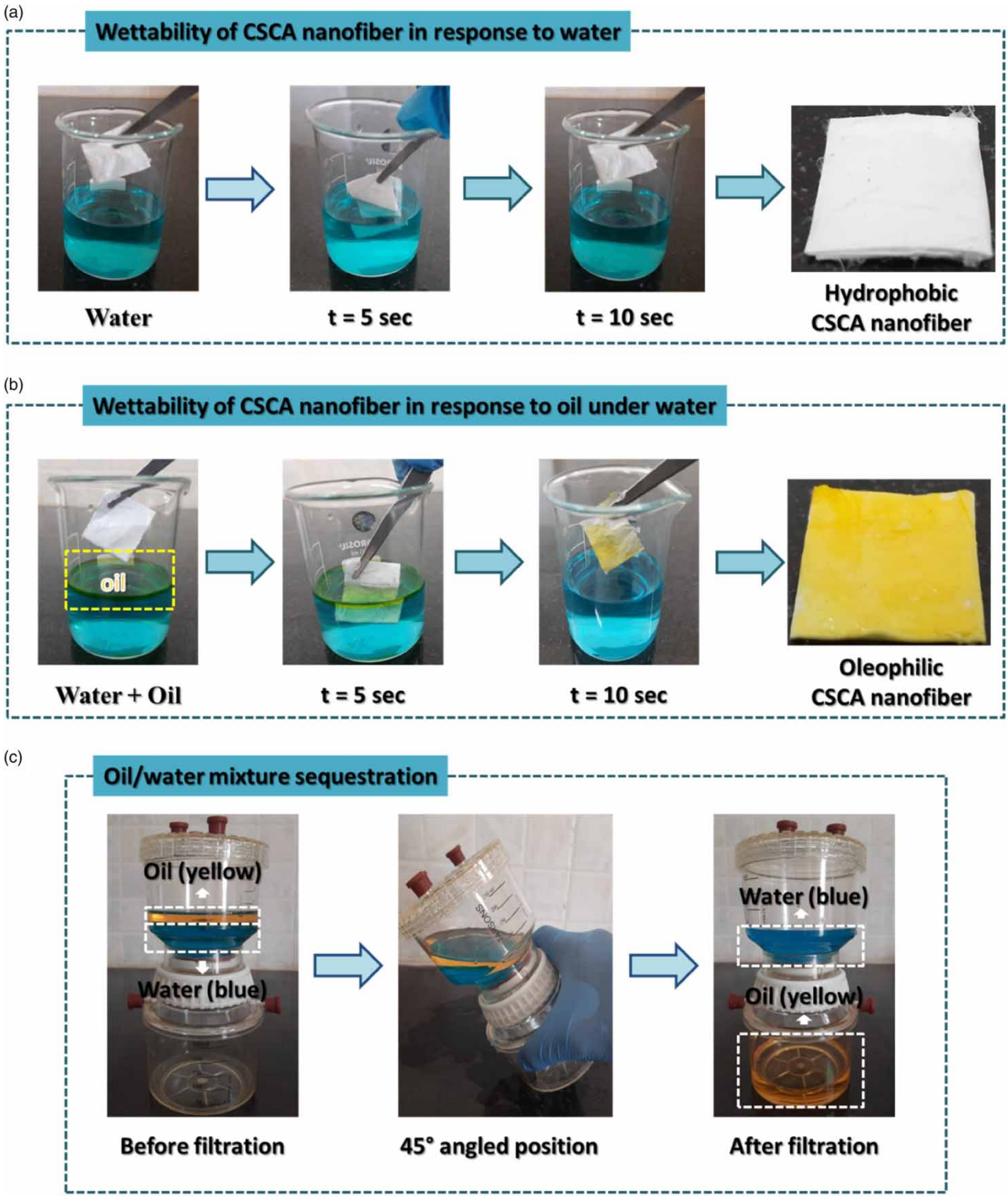

Figure 5 | (a) Wettability of CSCA nanofiber in response to water, (b) wettability of CSCA nanofiber in response to oil–water mixture, and (c) oil–water mixture sequestration in a cross-flow filtration system.

particular, the oil sorption capacities of diesel oil, petrol, petroleum ether, toluene, and mineral oil were 842, 836, 778, 664, and 908%, respectively. The as-prepared CSCA membranes demonstrated the greatest sorption capacity to mineral oil, whereas their sorption capacity to toluene was the least. The high degree of ester compound present in the organic CSCA

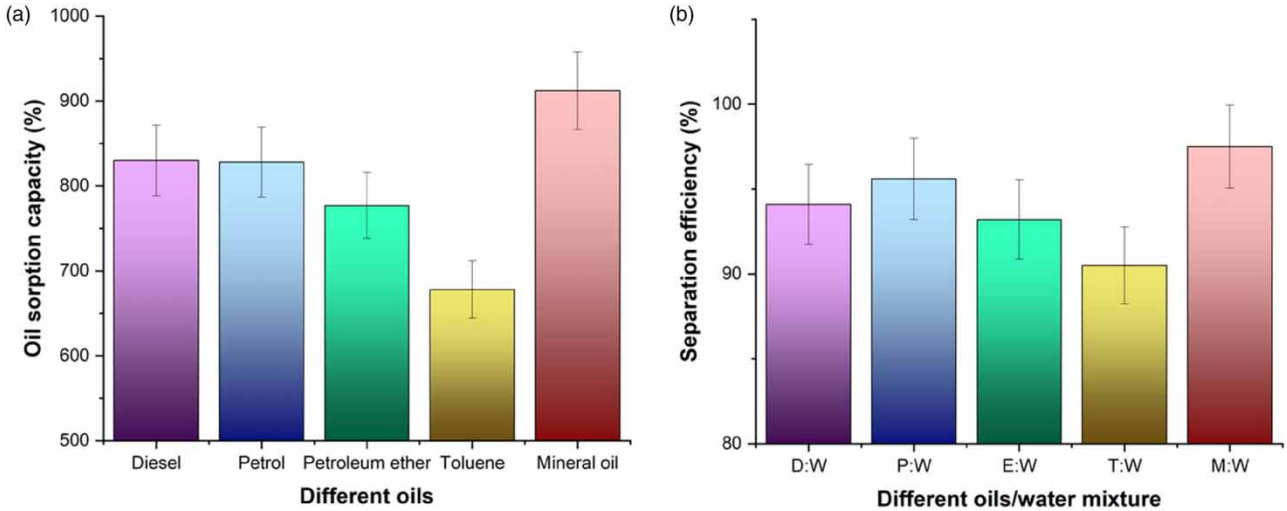

Figure 6 | (a) Oil sorption capacity for selected oils. (b) Separation efficiency of CSCA nanofiber membrane for different oil–water mixtures (diesel–water (D : W), petrol–water (P : W), petroleum ether–water (E : W), toluene–water (T : W), and mineral oil–water (M : W)).

membrane, together with its porous structure and huge pore volume, contributes significantly to this property. When tested with five different oil-and-water mixtures, the CSCA nanofiber membranes demonstrated a separation efficiency of more than 90% as displayed in Figure 6(b). In particular, the separation efficiencies of diesel–water (D : W), petrol–water (P : W), petroleum ether–water (E : W), toluene–water (T : W), and mineral oil–water (M : W) were 94.1, 95.6, 93.2, 90.5, and 97.6%, respectively. After being exposed to the elements for a long time, abandoned sorption materials that have not been properly disposed of can become brittle and fracture, releasing micro-pollutants into the soil. In order to remove oil from water, several different types of oil absorbents have been created during the past decade. Regrettably, the majority of research that has been conducted so far has concentrated on oil–water separation capabilities, but only a small number of studies have taken into consideration the end of life and disposal of sorption materials after they have been used. However, in this investigation, previously used membranes are reconstituted for many oil absorption test cycles. In order to regenerate the nanofiber membrane, the oil-loaded membrane needed to be manually squeezed to expel the majority of the absorbed oil and then be washed in 100% ethanol to get rid of any remaining oil residue. The mineral oil–water (M : W) mixture was selected for the subsequent trials since the membrane performed most efficiently when confronted with this specific kind of oil–water combination. The recyclable potential of the CSCA membrane underwent additional investigation. Figure 7(a) depicts the separation effectiveness of membrane and oil purity after each cycle up to 25 cycles. After 25 attempts of separation studies, the separation efficiency was still greater than 96%, and the resulting oily phase remained 99.6% pure. These results indicate that the CSCA nanofiber membrane for oil–water mixture separation has an excellent separation efficiency and stability in structure.

3.5. Oil–water emulsion sequestration

By using traditional techniques, it is significantly more challenging to separate an oil–water emulsion, particularly when surfactants are present. Oil–water emulsions may be effectively separated via membrane technology, especially when the particles of oil are substantially smaller than 10 μm. As a result, similar research on the CSCA membrane's capacity to cleanse oil–water emulsion was conducted utilizing a cross-flow filtration apparatus. With the exception of the apparatus being upright, the experiment was conducted similarly to the oil–water separation. The emulsion's own gravitational pull is mostly responsible for driving the separation process. Oil–water emulsions of various types (D : W, P : W, E : W, T : W, and M : W) were then separated using the CSCA nanofiber membrane. Figure 7(b) depicts the oil–water emulsion separation using various oils. The CSCA membrane showed the best rejection to M : W emulsion but a relatively lower rejection to diesel and petrol emulsion, because diesel and petrol were viscous and quickly closed the pores on nanofibers during the filtration process. The reason for this difference is that diesel and petrol were more difficult to reject. The separation fluxes of the CSCA membrane for oil–water (D : W, P : W, E : W, T : W, and M : W) emulsion are 434, 442, 418, 412, and 402 L/m^2/h, respectively. These results indicate that the more the viscosity of the fluid, the lesser the flux. Similarly, M : W emulsion was

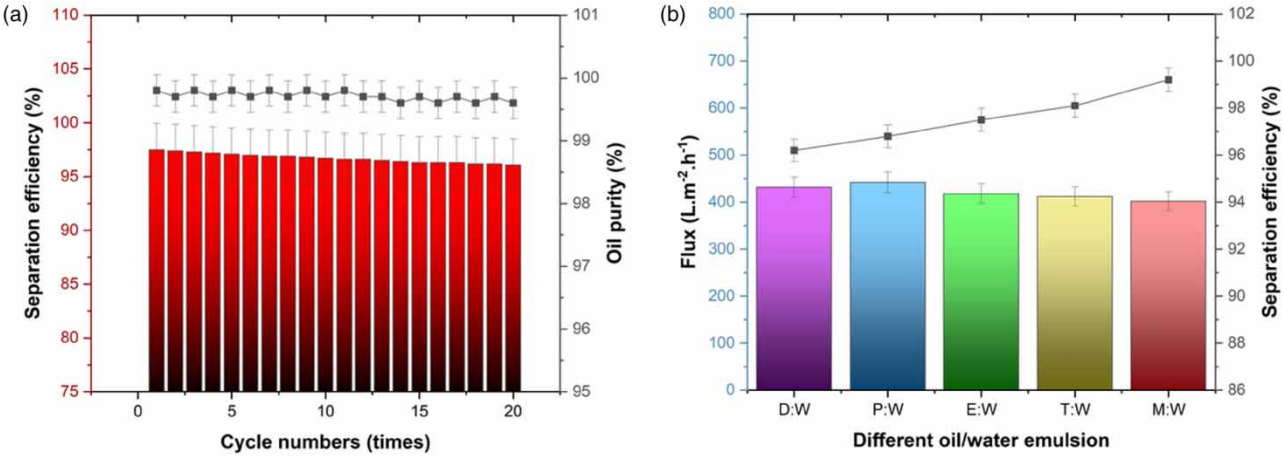

Figure 7 | (a) Separation efficiency and oil purity against cycle times. (b) Separation flux and efficiency against different oil–water emulsion (diesel–water (D : W), petrol–water (P : W), petroleum ether–water (E : W), toluene–water (T : W), and mineral oil–water (M : W)).

Table 1 | Comparison of electrospun nanofiber membranes for oil–water mixture separation

S. No.	Nanofiber membrane (NFM)	WCA (°)	Maximum separation flux (L/m^2/h)	Maximum separation efficiency (%)	References
1	Super amphilic-modified CA NFM	150	38,000	99.97	Wang *et al.* (2020b)
2	Superlyophobic cellulose NFM	–	3,000	99	Li *et al.* (2020)
3	Polylactic acid NFM	152	13,818	99.24	Ye *et al.* (2023)
4	*Metaplexis japonica* seed hair NFM	151.12	–	98	Wang *et al.* (2020c)
5	Ag nanoparticle-modified polyvinylidene fluoride (PVDF) NFM	152.5	11,000	99.2	Su *et al.* (2022)
6	Sugarcane bagasse ester-based NFM	142.1	419.8	99.54	Chen *et al.* (2022)
7	PVC/SiO_2/SiO_2@Ag NFM	153	166.48	95	Liu *et al.* (2022)
8	Polycaprolactone NFM	145	764	99.3	Dong *et al.* (2023)
9	Ag@sPEN NFM	144.8	3,597	98.3	Li *et al.* (2023)
10	CSCA NFM	156	442	97.5	This study

shown to have the highest separation efficiency, whereas D : W emulsion had the lowest. In addition, mineral oil is able to diffuse through the hydrophobic membrane under the influence of gravity, whereas water is rejected by the hydrophobic surface, resulting in a clear emulsion. The separation efficiency exhibited no apparent deviations and it is >95% for every type of oil–water emulsion. The foregoing findings demonstrate that the CSCA nanofiber membrane has high separation capability for oil–water emulsions stabilized by surfactants. Table 1 presents a comparative analysis of the performance of CA nanofiber membranes in relation to previously reported nanofiber membranes.

4. CONCLUSION

Cellulose was extracted from dried CS by using an integrated green pretreatment. Furthermore, through the acetylation of obtained cellulose, CA has been produced. Electrospinning was used to make CSCA nanofibers with a porous structure via blending with PAN. Because of the porous, hydrophobic, and oleophilic properties of the fibers, they are an excellent contender for the role of a sustainable oil sorbent. It was found that mineral oil had the highest oil sorption capacity at 908%, while toluene had the lowest at 664%. This result is four times greater than the oil sorption capacities of commercially

available oil sorbents. For all of the prioritized oil–water emulsions, the separation fluxes were higher than 400 L/m^2/h. In addition, the separation efficiency was >90% for all of the selected oil–water mixtures and >95% for oil–water emulsions. The separation efficiency was still higher than 96% after 25 cycles of separation experiments, and the resultant oily phase was still 99.6% pure, demonstrating exceptional potential for reuse. Because of the high surface porosity, the surface area of the fibers was significantly enhanced, which, in practice, implies that there was more contact area for the oil on the sorbent, which ultimately led to a high oil sorption capacity. The solution's viscosity is inversely proportional to its CA content. The bonding information in CA fiber may be understood by structural analysis. These membranes provide a low-priced, high-efficiency method for cleaning oil out of water. Still, challenges in managing nanofiber shapes continue. More work is needed, as well as novel methodologies, to efficiently design the surface morphology of nanofibers; this will pave the way for further exploration of fibrous materials and spur more study. As a consequence, the results confirmed that the CSCA membranes, due to their simple construction and enhanced properties, may be used by industries as an ecologically friendly and cost-competitive technology to separate oil from oil-contaminated industrial effluent.

DATA AVAILABILITY STATEMENT

All relevant data are included in the paper or its Supplementary Information.

CONFLICT OF INTEREST

The authors declare there is no conflict.

REFERENCES

Alvarado-Gómez, E., Tapia, J. I. & Encinas, A. 2021 A sustainable hydrophobic luffa sponge for efficient removal of oils from water. *Sustainable Materials and Technologies* **28**, e00273.

Araujo, D., Vilarinho, M. & Machado, A. 2019 Effect of combined dilute-alkaline and green pretreatments on corncob fractionation: pretreated biomass characterization and regenerated cellulose film production. *Industrial Crops and Products* **141**, 111785.

Asriza, R. O., Humaira, D. & Ryaldi, G. O. 2021 Characterization of cellulose acetate functional groups synthesized from corn husk (*Zea mays*). In *IOP Conference Series: Earth and Environmental Science* (Vol. 926, No. 1, p. 012060). IOP Publishing, Bristol, UK.

Bai, L., Wang, X., Guo, X., Liu, F., Sun, H., Wang, H. & Li, J. 2023 Superhydrophobic electrospun carbon nanofiber membrane decorated by surfactant-assisted in-situ growth of ZnO for oil–water separation. *Applied Surface Science* **622**, 156938.

Biswas, A., Saha, B. C., Lawton, J. W., Shogren, R. L. & Willett, J. L. 2006 Process for obtaining cellulose acetate from agricultural by-products. *Carbohydrate Polymers* **64** (1), 134–137.

Chen, W., Wang, H., Lan, W., Zhang, A. & Liu, C. 2022 Fabrication of sugarcane bagasse ester-based porous nanofiber membrane by electrospinning for efficient oil-water separation. *Industrial Crops and Products* **187**, 115480.

de Almeida, D. S., Duarte, E. H., Hashimoto, E. M., Turbiani, F. R., Muniz, E. C., de Souza, P. R., Gimenes, M. L. & Martins, L. D. 2020 Development and characterization of electrospun cellulose acetate nanofibers modified by cationic surfactant. *Polymer Testing* **81**, 106206.

Dong, T., Ye, H., Wang, W., Zhang, Y., Han, G., Peng, F., Lou, C. W., Chi, S., Liu, Y., Liu, C. & Lin, J. H. 2023 A sustainable layered nanofiber/sheet aerogels enabling repeated life cycles for effective oil/water separation. *Journal of Hazardous Materials* **454**, 131474.

Eleryan, A., El Nemr, A., Idris, A. M., Alghamdi, M. M., El-Zahhar, A. A., Said, T. O. & Sahlabji, T. 2021 Feasible and eco-friendly removal of hexavalent chromium toxicant from aqueous solutions using chemically modified sugarcane bagasse cellulose. *Toxin Reviews* **40** (4), 835–846.

Elmaghraby, N. A., Omer, A. M., Kenawy, E. R., Gaber, M. & El Nemr, A. 2022 Electrospun composites nanofibers from cellulose acetate/carbon black as efficient adsorbents for heavy and light machine oil from aquatic environment. *Journal of the Iranian Chemical Society* **19** (7), 3013–3027.

Embong, N. H., Hindryawati, N., Bhuyar, P., Govindan, N., Rahim, M. H. A. & Maniam, G. P. 2021 Enhanced biodiesel production via esterification of palm fatty acid distillate (PFAD) using rice husk ash ($NiSO_4$)/SiO_2 catalyst. *Applied Nanoscience* **13**, 1–9.

Fang, J., Zhang, G. & Meng, C. 2022 Natural recyclable high-efficiency oil-water separation and interfacial dye adsorption material: duck down fiber. *Journal of Natural Fibers* **19** (13), 6497–6508.

Ge, J., Zong, D., Jin, Q., Yu, J. & Ding, B. 2018 Biomimetic and superwettable nanofibrous skins for highly efficient separation of oil-in-water emulsions. *Advanced Functional Materials* **28** (10), 1705051.

Islam, M. S., Ang, B. C., Andriyana, A. & Afifi, A. M. 2019 A review on fabrication of nanofibers via electrospinning and their applications. *SN Applied Sciences* **1**, 1–16.

Israel, A. U., Obot, I. B., Umoren, S. A., Mkpenie, V. & Asuquo, J. E. 2008 Production of cellulosic polymers from agricultural wastes. *Journal of Chemistry* **5**, 81–85.

Kou, X., Han, N., Zhang, Y., Tian, S., Li, P., Wang, W., Wu, C., Li, W., Yan, X. & Zhang, X. 2021 Fabrication of polyphenylene sulfide nanofibrous membrane via sacrificial templated-electrospinning for fast gravity-driven water-in-oil emulsion separation. *Separation and Purification Technology* **275**, 119124.

Kovačević, A., Radoičić, M., Marković, D., Ponjavić, M., Nikodinovic-Runic, J. & Radetić, M. 2023 Non-woven sorbent based on recycled jute fibers for efficient oil spill clean-up: from production to biodegradation. *Environmental Technology & Innovation* **31**, 103170.

Li, X., Cao, M., Shan, H., Tezel, F. H. & Li, B. 2019 Facile and scalable fabrication of superhydrophobic and superoleophilic PDMS-co-PMHS coating on porous substrates for highly effective oil/water separation. *Chemical Engineering Journal* **358**, 1101–1113.

Li, Y., He, Y., Fan, Y., Shi, H., Wang, Y., Ma, J. & Li, H. 2020 Novel dual superlyophobic cellulose membrane for multiple oil/water separation. *Chemosphere* **241**, 125067.

Li, X., He, X., Ling, Y., Bai, Z., Liu, C., Liu, X. & Jia, K. 2023 In-situ growth of silver nanoparticles on sulfonated polyarylene ether nitrile nanofibers as super-wetting antibacterial oil/water separation membranes. *Journal of Membrane Science* **675**, 121539.

Liu, Y. 2020 *Development of Functional Flax Fibers Through Self-Assembled Nanoparticles for Oil-Water Separation*. The University of Regina, Canada.

Liu, H., Sun, Y., Xu, H., Qin, Y., Huang, Q., Chen, K., Shu, W. & Xiao, C. 2022 Dual-functional design of tubular polyvinyl chloride hybrid nanofiber membranes for the simultaneous oil/water separation and in-situ catalytic degradation. *Journal of Membrane Science* **661**, 120955.

Ma, Q., Cheng, H., Fane, A. G., Wang, R. & Zhang, H. 2016 Recent development of advanced materials with special wettability for selective oil/water separation. *Small* **12** (16), 2186–2202.

Mahmoud, M. A. 2020 Oil spill cleanup by raw flax fiber: modification effect, sorption isotherm, kinetics and thermodynamics. *Arabian Journal of Chemistry* **13** (6), 5553–5563.

Nemr, A. E., Ragab, S. & Sikaily, A. E. 2017 Rapid synthesis of cellulose triacetate from cotton cellulose and its effect on specific surface area and particle size distribution. *Iranian Polymer Journal* **26**, 261–272.

Prakash, J., Venkataprasanna, K. S., Bharath, G., Banat, F., Niranjan, R. & Venkatasubbu, G. D. 2021 In-vitro evaluation of electrospun cellulose acetate nanofiber containing graphene oxide/TiO_2/curcumin for wound healing application. *Colloids and Surfaces A: Physicochemical and Engineering Aspects* **627**, 127166.

Shu, D., Xi, P., Cheng, B., Wang, Y., Yang, L., Wang, X. & Yan, X. 2020 One-step electrospinning cellulose nanofibers with superhydrophilicity and superoleophobicity underwater for high-efficiency oil-water separation. *International Journal of Biological Macromolecules* **162**, 1536–1545.

Singh, C. J., Mukhopadhyay, S. & Rengasamy, R. S. 2023 A sustainable approach to oil spill cleanup by kapok and waste cotton needle punched nonwoven blends. *Industrial Crops and Products* **191**, 115939.

Sivashankar, R., Sivasubramanian, V., Kishore, K. A., Sathya, A. B., Thirunavukkarasu, A., Nithya, R. & Deepanraj, B. 2022 Metanil Yellow dye adsorption using green and chemical mediated synthesized manganese ferrite: an insight into equilibrium, kinetics and thermodynamics. *Chemosphere* **307**, 136218.

Su, R., Li, L., Kang, J., Ma, X., Chen, D., Fan, X. & Yu, Y. 2022 AgNPs-thiols modified PVDF electrospun nanofiber membrane with a highly rough and pH-responsive surface for controllable oil/water separation. *Journal of Environmental Chemical Engineering* **10** (5), 108235.

Trejo, M., Bhuyar, P., Velu, G., Pérez, E. Z., Unpaprom, Y., Trail, A. & Ramaraj, R. 2022 The effect of various pretreatments conditions on the distribution of fermentable sugar from dried elephant ear plant. *Fuel* **324**, 124624.

Wang, X., Yu, J., Sun, G. & Ding, B. 2016 Electrospun nanofibrous materials: a versatile medium for effective oil/water separation. *Materials Today* **19** (7), 403–414.

Wang, D., Yue, Y., Wang, Q., Cheng, W. & Han, G. 2020a Preparation of cellulose acetate-polyacrylonitrile composite nanofibers by multi-fluid mixing electrospinning method: morphology, wettability, and mechanical properties. *Applied Surface Science* **510**, 145462.

Wang, W., Lin, J., Cheng, J., Cui, Z., Si, J., Wang, Q., Peng, X. & Turng, L.-S. 2020b Dual super-amphiphilic modified cellulose acetate nanofiber membranes with highly efficient oil/water separation and excellent antifouling properties. *Journal of Hazardous Materials* **385**, 121582.

Wang, Z., Wang, D., Li, Z. & Wang, Y. 2020c Metaplexis japonica seed hair fiber: a hydrophobic natural fiber with robust oil–water separation properties. *Cellulose* **27**, 2427–2435.

Xue, J., Wu, T., Dai, Y. & Xia, Y. 2019 Electrospinning and electrospun nanofibers: methods, materials, and applications. *Chemical Reviews* **119** (8), 5298–5415.

Ye, Y., Li, T., Zhao, Y., Liu, J., Lu, D., Wang, J., Wang, K., Zhang, Y., Ma, J., Drioli, E. & Cheng, X. 2023 Engineering environmentally friendly nanofiber membranes with superhydrophobic surface and intrapore interfaces for ultrafast Oil-water separation. *Separation and Purification Technology* **317**, 123885.

Zhang, G., Wang, P., Zhang, X., Xiang, C. & Li, L. 2019 Preparation of hierarchically structured PCL superhydrophobic membrane via alternate electrospinning/electrospraying techniques. *Journal of Polymer Science Part B: Polymer Physics* **57** (8), 421–430.

Zhou, F., Wang, Y., Dai, L., Xu, F., Qu, K. & Xu, Z. 2022 Anchoring metal organic frameworks on nanofibers via etching-assisted strategy: toward water-in-oil emulsion separation membranes. *Separation and Purification Technology* **281**, 119812.

First received 6 July 2023; accepted in revised form 5 September 2023. Available online 16 September 2023